PHYSICAL REVIEW B VOLUME 26, NUMBER 12 15 DECEMBER 1982

High field conduction and dielectric breakdown in nominally pure and nickel-doped MgO crystals at high temperatures

K. L. Tsang
Department of Physics, University of Alabama, Birmingham, Alabama 35294
and Solid State Division, Oak Ridge National Laboratory, Oak Ridge, Tennessee 37830

Y. Chen
Solid State Division, Oak Ridge National Laboratory, Oak Ridge, Tennessee 37830

J. J. O'Dwyer
Department of Physics, S.U.N.Y., Oswego, New York 13126
(Received 18 February 1982; revised manuscript received 16 July 1982)

The phenomenon of dielectric (or more aptly, electrothermal) breakdown of nominally pure and nickel-doped MgO crystals at 1473 K is studied with the use of a field of 1500 $V\,cm^{-1}$. The current transients induced by constant and alternating fields as well as by field reversals, and open- and short-circuit conditions are investigated. Activation energies, obtained from the temperature dependence of current parameters, are also obtained. It is concluded that the mechanism leading to the breakdown involves the buildup of space charge caused by the injection of carriers from the electrodes and drift of ions.

I. INTRODUCTION

All solids conduct electricity and all suffer some form of breakdown in a sufficiently strong electric field.[1] In the case of insulators, it is commonly referred to as dielectric (or more aptly, electrothermal[2]) breakdown. It has been a subject of experimental and theoretical investigations for many years.[1] Nevertheless, there does not exist an unambiguous model for breakdown in ionic crystals, even though models for the conduction mechanisms of various materials occasionally arise.[1,3–20]

Most of the investigations of alkali-metal halides have focused on the breakdown strengths, near room temperature, under such high fields ($\sim 10^6$ V/cm) that breakdown occurred in milliseconds or less.[21–29] Hence, the study of the breakdown mechanism was difficult. In the case of refractory materials such as MgO crystals, there has been a dearth of research on the breakdown mechanism. Lewis *et al.* investigated MgO crystals at moderate temperatures (~ 800 K) with the use of high fields ($\sim 10^6$ V/cm) and suggested that electron (or hole) transport in conjunction with trapping might be responsible for the breakdown,[30,31] a suggestion similar to that by Hanscomb for NaCl and KCl crystals.[23] Sonder *et al.* suggested that the mechanism for breakdown of MgO crystals at ~ 1500 K using moderate fields ($\sim 10^3$ V/cm) is due to a resistivity decrease along pathways of $a\langle 100\rangle$ dislocations and small-angle grain boundaries, leading to breakdown.[32]

In this study moderate fields ($\sim 10^3$ V/cm) at high temperatures were used to achieve a near-breakdown condition in a reasonable laboratory time scale. In order to understand better the mechanism of breakdown, a detailed study of the electrical characteristics leading to the breakdown was undertaken (i.e., prebreakdown characteristics). MgO crystals were chosen as a prototype refractory material for an investigation on breakdown, because of the availability of well-characterized high-quality crystals and the simple crystal structure. Previous studies have revealed that breakdown in MgO crystals is impurity related and that it occurs in tens to hundreds of hours at ~ 1500 K with moderate fields ($\sim 10^3$ V/cm).[32–34] To understand the role that impurities may play in electrothermal breakdown, efforts were concentrated on nickel-doped MgO. Results for these crystals were compared with those of nominally pure MgO crystals. The purpose of the present investigation is to study the time-dependent current and to deduce a model for the breakdown phenomenon at high temperatures.

II. SAMPLE PREPARATION AND EXPERIMENTAL PROCEDURE

The MgO:Ni crystals used in this investigation were grown in the Oak Ridge National Laboratory

by an arc-fusion technique[35] using MgO powder from the Kanto Chemical Company, Tokyo, Japan, mixed with NiO powder. The crystals were found by spectrographic analyses to contain about 0.4 at. % nickel impurity. The results from optical and transmission electron-microscopy studies[36] indicate that notwithstanding the extraordinarily high concentration of nickel dopant in these crystals, only a very small percentage of the impurity is in precipitate form, and these precipitates are found to be associated with sub-boundaries. Voids and cracks were not observed. The nickel dopant is mostly dissolved as Ni^{2+} ions in the matrix.

Samples of dimensions $15\times15\times2.5$ mm^3 were prepared by cleaving and abrading along {100} planes from single-crystal ingots. The samples were then etched by chemical polishing in hot phosphoric acid maintained at 365 K. This procedure was taken to remove the damaged surface from which dislocations propagate into the crystal at elevated temperatures.[37]

The experimental setup is shown in Fig. 1. The sample is sandwiched between two flat circular platinum electrodes with a diameter of 6.3 mm and suspended in the hot zone of a vertical alumina furnace tube. Constant electric field was provided from a dc power supply (PRL CP-1413-V) and alternating electric field was generated by a line-to-line transformer (STANCOR P-4076) in conjunction with an autotransformer (VARIAC, W5MT3). Currents were monitored with a digital multimeter and also recorded by a strip-chart recorder. A variable resistor R_T was used in conjunction with the recorder to permit proper scaling. A fuse was used to protect the power supply. Temperatures were measured by Pt and Pt (10% Rh) thermocouples and did not fluctuate more than ±1 K.

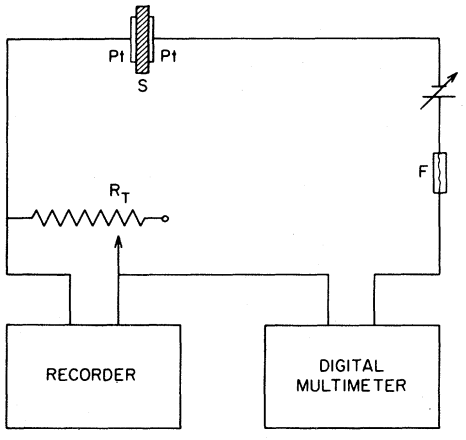

FIG. 1. Circuit diagram for the experiment on electrothermal breakdown.

All experiments in this study were performed with a constant field of 1500 V cm^{-1} applied across the MgO:Ni sample at 1473 K, unless stated otherwise. Pressure contacts using cylindrical platinum rods were used throughout, except that evaporated platinum contacts were used on one occasion and yielded the same results. All measurements were made by the two-probe method. In order to check the effect of surface conduction, a guarded electrode was used and no difference in current behavior was observed.

III. RESULTS

A. Current behavior with field reversals

When a field was applied to a sample at 1473 K, a current increase over many hours was observed. Typically when the current reached a given level, the field was reversed quickly and the current in the opposite direction was measured as a function of time. Usually, several reversals were made and the current behavior of a typical sample is shown in some detail in Fig. 2.

Field was applied at $t=0$, after the sample had been heated at 1473 K for about 10 min in order to ascertain that the sample temperature had reached equilibrium. The current initially decreased from 0.20 to 0.10 mA in 40 min (top inset), and then increased at an exponential rate until 18 mA was obtained. This value represents a 180-fold increase from the minimum current value. The time re-

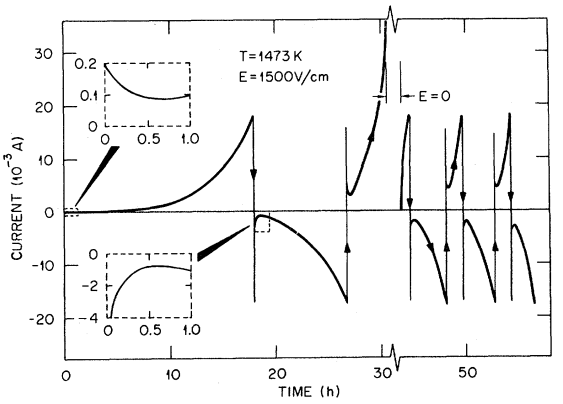

FIG. 2. Current vs time at 1473 K with $E=1500$ V cm^{-1} applied to a MgO:Ni crystal for several polarity reversals. At $t=31$ h, the fuse was burned out at $I\sim35$ mA; field was reapplied after 13 h. Upon reapplication of the same field, less time is required to reach a certain current level if the time interval without the field is short.

quired to reach 18 mA, to be referred to as the characteristic time for breakdown, was 18 h. In this study, 18 mA was chosen as the value at which field reversals were to take place, because it is a sufficiently high value to assure that breakdown is imminent, but excessive currents are avoided to maintain the system at the ambient temperature. Upon reversal, the initial current in the opposite direction was slightly less than 18 mA. It then decreased to a minimum value of 0.7 mA in 25 min (lower inset), followed by an exponential increase which was faster than that in the first cycle. The characteristic time was only 9 h. Several more field reversals were performed subsequently. The current behavior was similar to that of the first reversal, but the characteristic time tends to diminish with each reversal, until ultimately only 2 h were required. It is noteworthy that current fluctuations were larger in the first cycle than in subsequent reversals, within 5% and 2%, respectively. Figure 3 plots the characteristic time as a function of chronological reversals. To be sure, the characteristic time for one polarity exceeds the other between the third and the tenth reversal, but the trend is evident in Fig. 3. Five other MgO:Ni crystals were studied in a similar fashion. The results were similar to those shown in Figs. 2 and 3, although the values differ slightly.

The time-dependent currents for each of the reversals can be described accurately as the sum of two exponential terms

$$I(t)=I_{01}e^{-t/\tau_1}+I_{02}e^{t/\tau_2} \quad \text{for } t>0 \tag{1}$$

where I_{01}, I_{02}, τ_1, and τ_2 are positive constants, and $I_{01}>I_{02}, \tau_1<\tau_2$. The equation shows a minimum in $I(t)$ at a time denoted by t_m. At $t<t_m$, the first term, $I_{01}e^{-t/\tau_1}$, is predominant and therefore the current is decreasing. At $t>t_m$, the second term, $I_{02}e^{t/\tau_2}$, dominates.

Reversal experiments under identical experimental conditions were performed also on nominally pure MgO crystals. The current behavior was essentially the same as for MgO:Ni crystals, but the magnitude of the characteristic times were about 30% to 50% larger. The instantaneous current, $-I_{i0}$, after field reversal was smaller. The reversed current reached its minimum value in a much shorter time.

It is noted that when dc was applied to MgO:Ni, black streaks[34] propagating from the negative electrode were observed. Streaks were observed when the contacts were nonuniform. Good contacts were produced using chemically polished crystal, as evidenced by the uniform distribution of dark coloration. If the field was sustained for a sufficiently long time, most of the crystal between the electrodes became darkened. The coloration is in part due to collodial Ni. A broad optical-absorption band at ~ 2.2 eV is similar to that observed in reduced MgO:Ni crystals.[38] For undoped MgO crystals, no such coloration was observed.

Figure 4 illustrates the general current behavior in MgO:Ni crystals when polarity is reversed at different stages of a given cycle, where a cycle refers to the time interval between two field reversals performed at 18 mA. The solid curve at the bottom represents a given cycle when the field was initially reversed at t_1. The behavior of the current, when the polarity was reversed again at three different stages, such as t_2, t_3, and t_4, is illustrated in the figure and described as follows.

(i) Polarity switch at t_2, when the current was de-

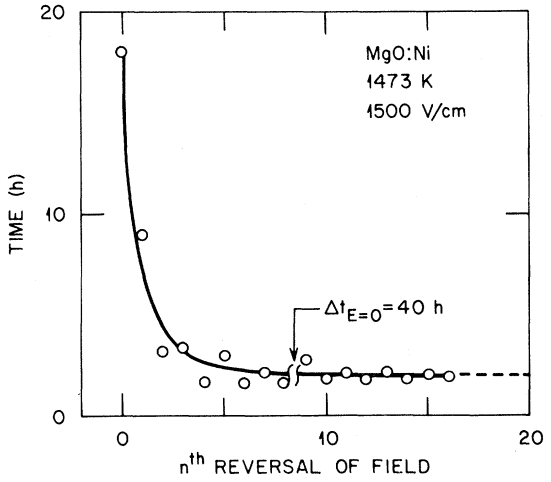

FIG. 3. Characteristic time for breakdown vs the nth field reversal.

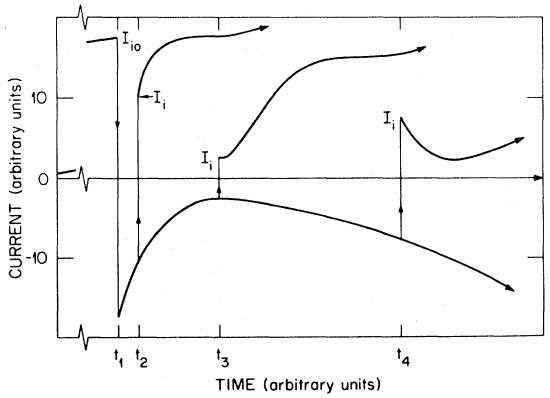

FIG. 4. Current behavior when the field is reversed at different stages of a given cycle.

creasing: Flowing in the opposite direction, the current reaches an instanteous value I_i, which has the same magnitude as the current prior to the polarity change. It then continues to rise and saturate at I_{i0} before embarking on an exponential increase.

(ii) Polarity switch at t_3, when the current was at a minimum: The current reverses and also rises immediately to an instantaneous value I_i with the same magnitude as the current prior to the polarity switch. The current remains at I_i for a short period before increasing. Subsequently the current levels off before embarking on the exponential course.

(iii) Polarity switch at t_4, when the current was increasing exponentially: An instantaneous current in the opposite direction is again observed. The subsequent current behavior is the same as that shown in Fig. 2.

Some generalizations on the current behavior in MgO:Ni crystals can be made from Fig. 4. Firstly, whether the current in a given cycle is decreasing, constant, increasing, polarity change will induce an instantaneous current, which has roughly the same magnitude as the current prior to the polarity switch but flows in the opposite direction. Secondly, the current behavior immediately following the instantaneous current will depend on the current prior to the polarity switch. A diminishing current will result by an increasing current, and vice versa. A constant current will be followed by a constant current. Thirdly, an exponential increase in current will ultimately occur.

B. Instantaneous current after time interval with $E=0$

An instantaneous current can be obtained in either direction upon restoration of the field following a time interval without applied field, to be denoted as $\Delta t(E=0)$. An illustration is shown in Fig. 5. An electric field was applied initially at $t=0$ and removed at $t=10$, when the current reached I_{i0}. When the same field was restored at $t=11$, an instantaneous current I_i was obtained. The subsequent current enhancement then slowed down at a level approximating I_{i0} before increasing exponentially. Later, if the field was removed at $t=12$ and a reversed field was applied at $t=13$, an instantaneous current in the opposite direction, $-I_i$, was obtained followed by a current behavior similar to that shown in Fig. 2.

The magnitude of the instantaneous current in either direction is a function of $\Delta t(E=0)$, shown in Fig. 6. Three initial currents, $I_{i0}=4.0$, 8.4, and 16 mA, in both directions are shown. The value of I_i decreased rapidly in the first minute and eventually reached a value which was nearly constant. It became nearly constant after 5 min for $I_{i0}<5$ mA, and 10 min for $I_{i0}>5$ mA. After 40 h (not shown), an instantaneous current $\simeq 0.5$ mA was detected for $I_{i0}=8.4$ mA. There appears to be symmetry between the positive and negative currents.

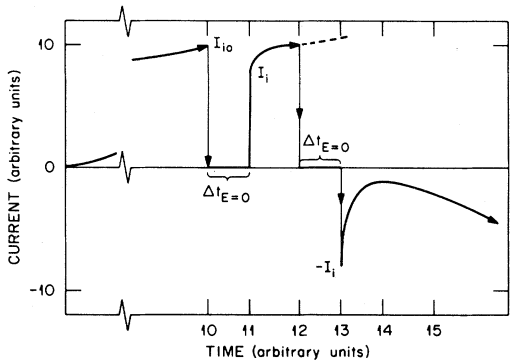

FIG. 5. Current behavior after a time increment without field ($\Delta t_{E=0}$). Instantaneous current I_i is the current obtained immediately (<1 sec) after reapplication of the field, either in the same or reversed direction.

C. Short-circuit current

A method of obtaining information on the distribution of stored charges inside the sample and therefore the mechanism of electrothermal breakdown is to measure the short-circuit current I_{sc}, which flows from one sample surface to the other via an external conductor when the electric field is removed. The I_{sc} as a function of time after field

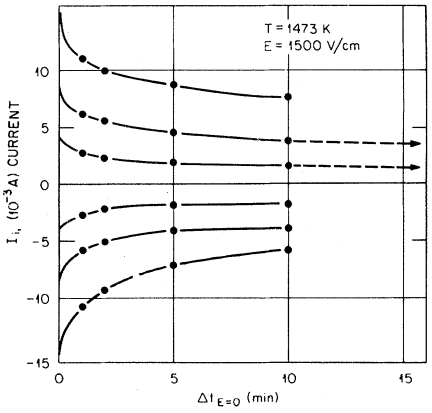

FIG. 6. Instantaneous current, I_i, as a function of time interval without field, $\Delta t_{E=0}$, for three different initial currents.

removal at $I_{i0}=+18$ mA is shown in the bottom of Fig. 7. It was found to flow in the opposite direction. It decreased rapidly in the first minute and remained nearly constant thereafter. For comparison, a curve for instantaneous current as a function of $\Delta t(E=0)$ is plotted in the top figure. While the shape of the I_{sc} and I_i curves appear to be symmetric, the former is about 3 orders of magnitude smaller.

When the same electric field was restored at $t=10$ min, an instantaneous current I_i of the same magnitude as that shown in the top curve was obtained. In fact, it would coincide with the top curve regardless of when the same field was applied again. Furthermore, higher I_{i0} results in higher I_{sc}. The coincidence of the I_i with the top curve and the small I_{sc} values indicate that annihilation of stored charges occur almost entirely within the crystal.

It is noted that immediately after field removal at $I_{i0}=18$ mA, a high-impedance voltmeter measured ~ 2 V across the sample with the polarity being the same as the applied field. The decay pattern of the voltage was similar to that of I_{sc}.

D. Alternating electric field

As noted in Fig. 2, it requires about an hour to observe a definite increase in current, and it requires 18 h for the current to reach 18 mA. Also investigated was the question of whether a similar current increase would occur if the same field was applied, but reversed frequently such as in an alternating electric field.

An alternating field of 1500 V cm^{-1} (rms),60 Hz, was applied to two samples: (a) an as-grown MgO:Ni crystal, and (b) a MgO:Ni crystal which had undergone a current increase due to direct bias. In the first sample there was no significant change in the current even after 24 h, even though there were fluctuations during the first 3 h (see lower curve in Fig. 8). No dark coloration across the sample was observable. In the second sample, the direct current through the sample reached 18 mA before the alternating field was applied. A high ac was observed initially (top curve) but it eventually decayed to a level somewhat higher than in the first case. The application of an alternating field did not appear to have removed the dark coloration caused by the direct bias.

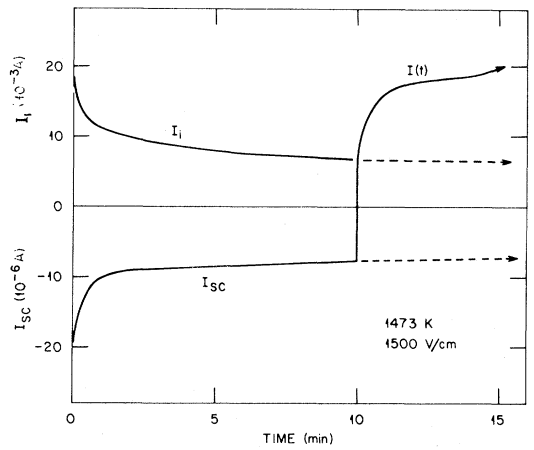

FIG. 7. Top curve: instantaneous current vs $\Delta t_{E=0}$. Bottom curve: short-circuit as a function of time.

E. Activation energy

The activation energy associated with the electrothermal breakdown of MgO crystals can be obtained by three different methods described as follows:

(a) *Time constants for* $I(t)$. As noted in Eq. (1), the time-dependent current $I(t)$ can be expressed as the sum of two exponential terms with different time constants. The characteristic time effectively diminishes with each reversal until a constant value is reached, as shown in Figs. 2 and 3. Correspondingly, the constants I_{01}, I_{02}, τ_1, and τ_2 are changing with each reversal. After the tenth reversal they remain unchanged. Activation energies associated with τ_1 and τ_2 after the tenth reversal were obtained: measurements were made at $T=1200$, 1248, 1302, and 1352 °C, as shown in Fig. 9. For a given field, the time constants τ_1 and τ_2 were found to obey the relationship

$$\tau_1=\tau_{01}e^{Q_1/kT}, \tag{2}$$

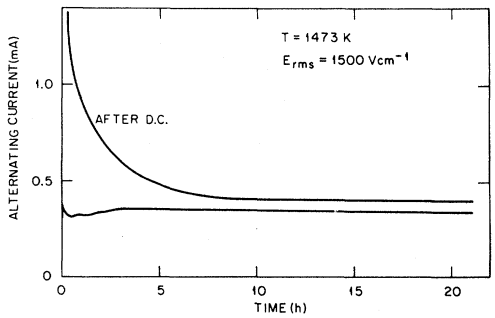

FIG. 8. Current vs time with application of alternating field for (a) an as-grown MgO:Ni crystal, and (b) a similar crystal having experienced a current increase due to a dc field.

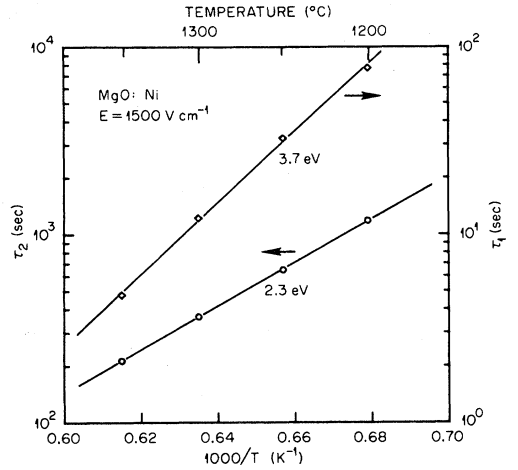

FIG. 9. $\log_{10}$ of the time constants τ_1 and τ_2 were plotted against $1000/T$. Activation energies determined from the slopes for τ_1 and τ_2 were 3.7 ± 0.3 eV and 2.3 ± 0.2 eV, respectively.

$$\tau_2=\tau_{02}e^{Q_2/kT}, \tag{3}$$

where Q_1 and Q_2 are activation energies for τ_1 and τ_2, respectively. The activation energies are $Q_1=3.7\pm0.3$ eV and $Q_2=2.3\pm0.2$ eV.

(b) *Short-circuit current.* Short-circuit current $I_{sc}(t)$ decreases rapidly in the first minute, but becomes nearly constant after 10 min (see Fig. 7). Therefore, the current can be measured at different temperatures (all within 5 min) when the temperature is cooling down. The results are shown in Fig. 10. Both the nickel-doped and the nominally pure MgO crystals yield an activation energy of 2.4 ± 0.1 eV.

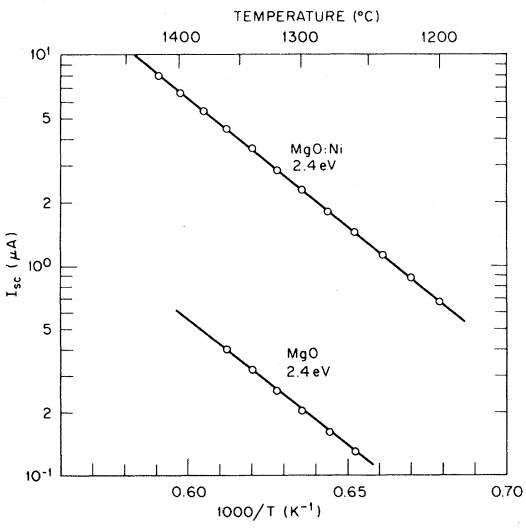

FIG. 10. $\log_{10}$ of the short-circuit current vs $1000/T$ for both MgO:Ni and nominally pure MgO crystals. Activation energy 2.4 ± 0.1 eV was obtained.

(c) *Alternating current.* As shown in Fig. 8, the alternating current becomes constant after 3 h of applied field. Therefore the temperature dependence of the steady-state current can be measured easily. The log of the alternating current plotted against $1000/T$ is shown in Fig. 11. An activation energy of 2.4 ± 0.1 eV was obtained.

IV. DISCUSSION AND CONCLUSIONS

In general, the current behavior of nominally pure and nickel-doped MgO crystals is similar, while the main difference between them is the time scale. We conclude that the mechanism for high field conduction and electrothermal breakdown in these two crystals is basically the same. In what follows we postulate a model for the conduction process that, while undoubtedly not unique, does offer a reasonable and consistent picture of the observed phenomena.

In the first place, it seems that the high-current levels observed (18 mA from an electrode of 0.30 cm^2 area corresponds to a current density of 60 mA/cm^2) must be explained in terms of two-carrier (electron and hole) current flow. Treating the current as ionic would require impossibly large concentrations of ions for any reasonable mobility value, and treating it as single carrier space charge

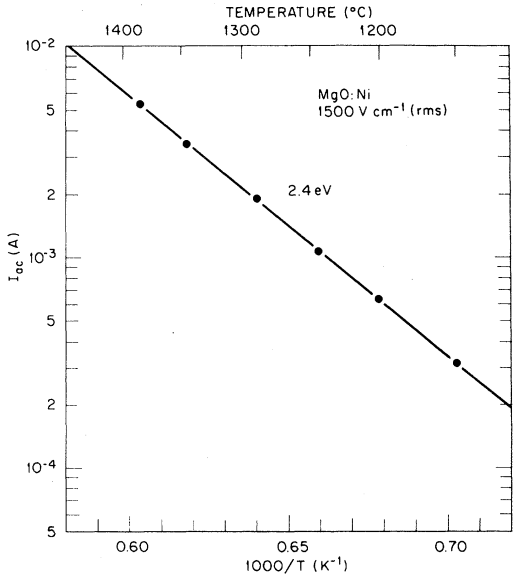

FIG. 11. $\log_{10}$ of the alternating current vs $1000/T$ for MgO:Ni crystal. Constant field 1500 V/cm (rms) was used. Activation energy 2.4 ± 0.1 eV was calculated from the slope.

limited (electron or hole) would result in a voltage several orders higher than the observed value for any reasonable mobility. The model proposed assumes that the dielectric initially contains n_0 relatively mobile free electrons, and an equal number of p_0 of highly immobile (trapped) holes. The platinum electrodes are assumed to provide an Ohmic contact for electrons and a very weakly injecting contact for holes. In the subsequent discussion electron-hole recombination is assumed to be very small.

Application of a voltage then causes a current of injected electrons. If we assume a relatively low level of injection, then $J = n_0 e\mu_n E \approx p_0 e\mu_n E$; taking an electron mobility of 10 $cm^2/V\,s$ the initial current density of 0.67 mA/cm^2 then requires a trapped hole density of 2.8×10^{11} cm^{-3}. The problem has been solved in detail by Lampert and Mark[39]; referring to their solution we calculate the dimensionless parameter

$$w_a = \frac{e^2 n_0^2 \mu_n L}{\epsilon J} = 8.5 \tag{4}$$

using a value of 10 for the dielectric constant. This value of w_a places the conduction in an Ohm's-law region.

The subsequent variation of current with time takes place very slowly, and we therefore treat the problem as a sequence of quasiequilibrium states. Figure 2 shows that the current decreases by a factor of 2 in about 30 min, and this requires a corresponding decrease in the trapped-hole density. This is readily accounted for by a drift of the trapped holes (and their eventual removal at the cathode) with a concomitant failure of the anode to inject sufficient replacements. This explanation would require a transit time for trapped holes of order of 30 min which would correspond to a mobility of about 10^{-7} $cm^2/V\,s$. The data of Fig. 9 showing an activiation energy of 3.7 eV associated with τ_1 lead us to believe that the hole mobility is associated with the same activation energy.

The subsequent large increase in current by a factor of 100 over the initial value requires, by the same argument, a similar increase in the trapped-hole density. Since the increase must take place over many hours, we propose that hole injection from the anode is substantially increased by slow accumulation of negatively charged ionic species (or vacancies) adjacent to that electrode. Using Poisson's equation we estimate that a constant ion density of 3.3×10^{12} cm^{-3} in the region 25-μm thick adjacent to the anode would double the field strength there. Checking once again with the Lampert and Mark[39] solution shows that these conditions are well within the Ohm's-law regime. Since Fig. 9 shows an activation energy of 2.3 eV associated with the time constant τ_2, we assume that the mobility of the ionic species in question is associated with the same activation energy.[20]

The model also offers excellent explanations of the behavior on voltage reversal (Figs. 2 and 4) and removal and reapplication of voltage (Fig. 5). Since the trapped-hole density is assumed to be quasisteady at all times, and since it dictates the value of the injected-electron current, simple voltage reversal should result in the same current in the opposite direction; this is observed in the experiments illustrated in Figs. 2 and 4. Moreover, since the new anode is now only weakly injecting, the current should decay in time of order of the hole transit time before it builds up to a large value as the negative ionic species slowly accumulate near the new anode. If the voltage is removed for some time before being reapplied, it is expected that the hole concentration will decay slowly towards its equilibrium value. Reapplication of the voltage should therefore cause a reduced current as observed in Fig. 5 ($I_i < I_{i0}$). Some idea of the rate of recombination that is required to explain the reduced current is given by the data shown in Fig. 6. If the voltage is reapplied in the same direction, the current should subsequently increase since much of the negative ionic charge remains adjacent to the anode. For voltage reapplication in the opposite direction, the current should decrease before it again increases since the new anode now is not adjacent to the residual negative charge. These conclusions are also in agreement with the data of Figs. 4 and 5.

The charge released during short circuit of the sample cannot be explained in terms of our current conduction model. The amount of charge released in 10 min after short circuit is about 6 mC (see Fig. 7), while the total charge (of either sign) supporting conduction is some 10 orders of magnitude lower. We are led to the conclusion that the long-time application of the field has resulted in the creation of a small and inefficient battery. The direction of the short-circuit current and the measured open-circuit voltage of the sample after a long period of conduction both support this conclusion.

Application of an ac voltage causes a current that is of similar magnitude to the initial current in the dc case; this is just what we would expect since the time of a voltage reversal is so short that none of

the effects described above have time to begin. Figure 11 shows that the ac conductivity follows an Arrhenius-type law with an activation energy of 2.4 eV.

In the experiments recorded, the sample was not allowed to proceed to breakdown since this would have destroyed it. However, several samples were tested to destruction, and broke down when the current rose an order of magnitude or more than the maximum allowed before voltage reversal. It is of interest to estimate the current density required for thermal breakdown at the constant voltage of the experiments. We assume that the temperature dependence of the electrical conductivity at high-current levels follows the Arrhenius-type law that we found for ac conduction. The critical thermal voltage is then given by[1]

$$V_c^2=\frac{8KkT_0^2}{\phi\sigma}\ , \tag{5}$$

where K is the thermal conductivity, ϕ the conduction activation energy, and σ the electrical conductivity at ambient temperature. Using known values for all other quantities we calculate $\sigma\sim 4.5\times 10^{-4}$ Ω^{-1} cm^{-1} at the onset of thermal breakdown. For the maximum allowed current in the experiments we find $\sigma\sim 4\times 10^{-5}$ Ω^{-1} cm^{-1}, so that our theoretical estimate also puts the onset of thermal breakdown at a current 1 order of magnitude higher than 18 mA.

ACKNOWLEDGMENTS

One of us (K.L.T.) is indebted to the University of Alabama at Birmingham for a fellowship. Discussions with M. M. Abraham, J. R. McDonald, F. A. Modine, E. Sonder, H. T. Tohver, J. C. Wang, and R. A. Weeks have been helpful. This research was sponsored by the Division of Materials Science, U. S. Department of Energy, under Contract W-7405-eng-26 with Union Carbide Corporation.

[1]J. J. O'Dwyer, *The Theory of Electrical Conduction and Breakdown in Solid Dielectrics* (Oxford University Press, Oxford, 1973).
[2]H. J. Wintle, J. Appl. Phys. 52, 4181 (1981).
[3]S. P. Mitoff, J. Chem. Phys. 31, 1261 (1959).
[4]S. P. Mitoff, J. Chem. Phys. 36, 1383 (1962).
[5]S. P. Mitoff, J. Chem. Phys. 41, 2561 (1964).
[6]Y. Oishi and W. D. Kingery, J. Chem. Phys. 33, 905 (1960).
[7]M. O. Davies, J. Chem. Phys. 38, 2047 (1963).
[8]N. A. Surplice and R. P. Jones, Brit. J. Appl. Phys. 15, 639 (1964).
[9]S. R. Pollack, J. Appl. Phys. 34, 877 (1963).
[10]P. R. Emtage and J. J. O'Dwyer, Phys. Rev. Lett. 16, 356 (1966).
[11]S. C. Jain and G. D. Sootha, J. Phys. Chem. Solids 26, 267 (1965).
[12]S. C. Jain and G. D. Sootha, Phys. Rev. 171, 1075 (1968).
[13]S. C. Jain and V. K. Jain, Phys. Rev. 181, 1312 (1969).
[14]A. E. Hughes and S. C. Jain, Adv. Phys. 28, 717 (1979).
[15]R. Straton, J. Phys. Chem. Solids 23, 1177 (1962).
[16]T. E. Hartman and J. S. Chivian, Phys. Rev. 134, A1094 (1964).
[17]D. R. Lamb, *Electrical Conduction Mechanism in Thin Insulating Film,* (Methuen, London, 1967).
[18]M. Lenzlinger and E. H. Snow, J. Appl. Phys. 40, 278 (1969).
[19]W. D. Kingery, H. K. Bowen, and D. R. Uhlmann, *Introduction to Ceramics,* 2nd ed. (Wiley, New York, 1976).
[20]D. R. Sempolinski, Ph.D. thesis, Massachusetts Institute of Technology, 1979 (unpublished).
[21]J. R. Hanscomb, Aust. J. Phys. 15, 504 (1962).
[22]J. R. Hanscomb, Brit. J. Appl. Phys. (J. Phys. D) 2, 1327 (1969).
[23]J. R. Hanscomb, J. Appl. Phys. 41, 3597 (1970).
[24]J. R. Hanscomb, K. C. Kao, J. H. Calderwood, J. J. O'Dwyer, and P. R. Emtage, Proc. Phys. Soc. London 88, 425 (1966).
[25]J. Lynn Smith and Paul P. Budenstein, J. Appl. Phys. 40, 3491 (1969).
[26]D. B. Watson and W. Heyes, J. Phys. Chem. Solids 31, 2531 (1970).
[27]R. Cooper, R. M. Higgin, and W. A. Smith, Proc. Phys. Soc. London Sect. B 76, 817 (1960).
[28]R. Cooper and C. T. Elliott, Brit. J. Appl. Phys. 17, 481 (1966).
[29]R. Cooper and D. L. Pulfrey, J. Phys. D 4, 292 (1971).
[30]T. J. Lewis and A. J. Wright, J. Phys. D 1, 441 (1968).
[31]T. J. Lewis and A. J. Wright, J. Phys. D 3, 1329 (1970).
[32]E. Sonder, K. F. Kelton, J. C. Pigg, and R. A. Weeks, J. Appl. Phys 49, 5971 (1978).
[33]R. A. Weeks, E. Sonder, J. C. Pigg, and K. F. Kelton, J. Appl. Phys. Suppl. C7, 411 (1976).
[34]F. A. Modine, L. A. Boatner, M. M. Abraham, W. P. Unruh, and R. Bunch, Bull. Am. Phys. Soc. 24, 413 (1979).
[35]M. M. Abraham, C. T. Butler, and Y. Chen, J. Chem. Phys. 55, 3752 (1971).
[36]J. Narayan and Y. Chen. J. Appl. Phys. 51, 1242

(1980).
[37]Y. Chen, N. Dudney, J. Narayan, and V. M. Orera, Philos. Mag. 44, 63 (1981).
[38]J. Narayan, Y. Chen, and R. M. Moon, Phys. Rev. Lett. 46, 1491 (1981).
[39]M. A. Lampert and P. Mark, *Current Injection in Solids* (Academic, New York, 1970).